Evaluation of Existing Crack Width Prediction Models for RC Panels with HSS Transverse Reinforcement

Morteza Hagh[1], Stephen J. Foster[2], Hamid Vali Pour[2], and Evan C. Bentz[3]
[1] Ph.D. Candidate, University of New South Wales
[2] Professor of Structural Engineering, University of New South Wales
[3] Professor of Civil Engineering, University of Toronto

Abstract: Leading design codes provide models for predicting flexural and tensile crack widths of reinforced concrete (RC) members but fall short of a prediction model for determining shear crack widths. The absence of a reliable model for shear cracks not only affects serviceability in conventionally reinforced members but also presents a barrier to integrating eco-efficient materials, such as high-strength steel (HSS), into the design of concrete structures. As a result, the Australian Standard (AS3600-2018) limits the yield strength of stirrups to 500 MPa for reinforcement if crack widths are not checked, and recommends that for strengths greater than 500 MPa, crack widths be checked using a suitably validated model, with no particular model being specified.

To address this gap, this study examines the applicability of existing crack width prediction models in reliably determining the widths of diagonal cracking of panels tested in pure shear. An iterative analysis is proposed to characterise service cracking behaviour in elements with HSS from existing panel data without the need for extensive testing. Selected shear crack models in the literature and the design standards are then evaluated against a dataset comprised of 113 reinforced concrete panel tests representative of elements with transverse HSS reinforcement. The results indicate that current models overestimate diagonal crack widths by at least 44%, which inhibits the adoption of HSS in practice due to perceived serviceability concerns. Subsequent modelling compatible with the Australian Standard's existing formulae is recommended to inform service limit state design of RC structures and facilitate the integration of HSS as an eco-efficient stirrup material.

Keywords: Diagonal Cracking, High-strength Steel, Crack Width Model, Shear Serviceability, RC Panel.

1. INTRODUCTION

High-strength steel (HSS) reinforcement is emerging as a key innovation in economical and sustainable design of reinforced concrete (RC) structures. In addition to offering higher strengths, incorporating HSS reinforcement can lower material costs by up to 11% (1). From a sustainability perspective, using less material translates to lower embodied carbon, considering the effects of material transportation and lighter construction (2). In a recent study, substituting HSS for mild steel in RC columns of a 19-story building in NSW resulted in a 16.7% reduction in embodied carbon (3). Other studies suggest that even larger reductions in the environmental impact of up to 45% could be achieved by utilising HSS in construction (4).

Despite the eco-economic advantages of HSS, current design code provisions for their use remain under development and require calibrated, material-specific design models (5). One key area of improvement is the provision of shear crack widths under the service limit state (SLS). In the absence of an acceptable crack width prediction model, design codes often limit the yield strength of shear reinforcement. For instance, the American Concrete Institute (ACI 318) does not allow the use of HSS as shear reinforcement unless in the form of wires with smaller diameters, in which case the strength can be up to 550 MPa. This highlights a lack of a reliable crack control model (6,7). Similarly, the Australian Standard (AS3600) limits the yield strength of stirrups to 600 MPa reinforcement if crack widths are checked, for which no models are suggested (8).

In studying the serviceability design of beams, Foster et al. (9) observed that existing models, primarily calibrated against flexural and tensile cracking in elements with mild steel, tend to consistently overestimate shear crack widths by as much as 60% when HSS stirrups are used. This significant overestimation would erroneously associate inadequate crack control with HSS stirrups, potentially inhibiting their practical use. Adopting HSS as a shear reinforcement thus necessitates a refined investigation targeting diagonal shear cracking in elements containing HSS, as undertaken in this study. To better assess and improve current prediction models, it is also essential to evaluate diagonal shear cracks in elements isolated from flexural effects.

While beam elements serve as a validation in serviceability models, many shear formulations in the literature are initially based on panel tests to yield strong analytical models. This approach is mainly due to the uniform strain conditions, which isolate shear cracks from the influence of other force actions. As such, panels can directly represent web-shear behaviour of RC beams and can be modelled as elements taken from a thin-web girder centroid at points of contraflexure (10). This makes panels valuable for studying diagonal shear cracking behaviour. Accordingly, this study utilises RC panels tested in pure shear to assess existing crack width formulations and inform subsequent modelling efforts centred on HSS.

Most shear panel tests available in the literature, however, comprise concrete elements reinforced with conventional steel. A review of pure shear panel experiments reveals that only 7% contain HSS in both longitudinal and transverse directions, with none featuring HSS solely as transverse reinforcement. Consequently, existing semi-empirical crack width formulations, calibrated against these tests, target the serviceability range observed for elements with reinforcement yield strengths up to 500 MPa (9). Any further extension to higher strengths would require substantial testing, which may be impractical due to the complexity and cost of pure shear test setups. To promote a fair representation of higher strengths, this study adopts an alternative approach that captures the service-level cracking behaviour of HSS-reinforced members using existing experimental data through an iterative analysis.

2. METHODOLOGY

2.1 Panel Data Collection

To establish a robust experimental benchmark for assessing existing crack width models, a dataset of pure shear experiments is compiled from the literature. This dataset encompasses over 150 load stages recorded across 47 conventionally reinforced concrete panel experiments conducted between 1981 and 2018 at the University of Toronto, the University of Houston, and ETH Zurich (11–22). The panels were reinforced in both the longitudinal and transverse directions and subjected to pure shear loading, resulting in diagonal shear cracks that formed without the influence of other force components.

It is worth noting that the dataset is limited to load stages occurring before the yield of reinforcement for two primary reasons. First, the similitude of HSS and conventional steel holds only within the linear elastic range, beyond which yielding leads to crack localisation that cannot be directly modelled. Second, according to AS3600 and other standards, stirrup yielding is not expected at the serviceability limit state. Therefore, the dataset includes only load stages within the linear elastic range of transverse steel, from which those representative of HSS behaviour are selected using the method outlined below.

2.2 HSS Representation

It is recognised that conventional and high-strength steel exhibit a similar constitutive behaviour within the linear elastic range, up to the yield strength of mild steel. However, for elements containing HSS, the serviceability limit state occurs at higher strains. If the higher steel strain at service remains within the elastic range of an equivalent conventionally reinforced element, the cracking behaviour of the two can be considered comparable. This assumption is based on the premise that bond behaviour – governed by rib configuration, diameter, and reinforcement ratio – remains unchanged. With this simplification, existing shear panel data can be used to represent the cracking behaviour of high-strength steel reinforced elements.

The compiled panel dataset, which is mainly comprised of conventionally reinforced elements, is analysed to identify load stages equivalent to the SLS condition of high-strength steel. First, the material and geometric properties of each panel are replicated in equivalent elements, but with a specified yield strength of the transverse reinforcement ranging from 550 MPa to 800 MPa. This range covers the typical yield strengths of commercially available HSS, with characteristic values up to 750 MPa. For a comparison rooted in crack mechanics, the strains of these HSS-equivalent elements, both concrete and steel, are then determined at service and subsequently matched against corresponding experimental data.

To achieve this, the stress and strain state of panel elements at SLS must be computed for each panel. Foster et al. previously developed an iterative procedure for beam elements, in which equilibrium, compatibility, and constitutive laws were established according to the Modified Compression Field Theory and conforming to AS3600 (8,9,19). This method enables estimation of the stress/strain state of beams at a given design service load. In this study, a similar approach is adopted and extended to panel elements to estimate concrete and steel strains at service loads defined as 40% to 60% of nominal strength. A detailed, step-by-step outline of this SLS iterative procedure with modifications to suit panel elements is provided in the appendix.

Once the SLS conditions of these panels are determined, the transverse steel and concrete principal tensile strains are matched to the corresponding data in the shear panel dataset. This ensures a direct equivalence can be drawn between mild and HSS reinforcement, considering the key strain variables influencing crack formation. As a result, 113 experimental data points are matched to represent the serviceability of shear panels reinforced with high-strength transverse steel and are used to evaluate existing crack width prediction models from the literature and leading design standards.

2.3 Existing Diagonal Crack Width Prediction Models

Table 1 outlines the four models selected for evaluation in this study. This includes two shear frameworks, the MCFT and the CMM, featuring semi-analytical crack models (23, 24). The evaluation herein also includes Eurocode's calibrated model for shear cracking and an extended version of the Australian Standard's model developed for flexure and adapted here to estimate shear crack widths (8, 25). This extension acknowledges, however, that the mechanisms and governing parameters for shear and flexural crack width development can differ significantly.

Table 1. Evaluated Crack Prediction Models.

<table>
<tr><th>Crack Spacing Model</th><th>Diagonal Crack Spacing Model</th><th>Crack Width Model</th><th>Parameter Definitions</th></tr>
<tr><td>Collins & Mitchell (1997) / MCFT
$s_{x,y\ avg} = 2\left(c + \frac{s}{10}\right) + 0.25\ k_1 \frac{d_b}{\rho_{s,\text{eff}}}$</td><td rowspan="2">$s_{\theta,avg} = \frac{1}{\left(\frac{sin\ \theta_{cr}}{s_{x,avg}} + \frac{cos\ \theta_{cr}}{s_{y,avg}}\right)}$</td><td rowspan="2">$w_{avg} = s_{\theta,avg}\ \varepsilon_1$</td><td rowspan="4">$\theta_{cr}$: Crack inclination w.r.t the longitudinal direction.
k_1, k_b: Bond quality. For deformed bars, it is taken as 0.4 for MCFT, 0.9 for Eurocode, and 0.8 for AS3600.
k_{fl}, k_2: Strain distribution and taken as 1.0 for pure tension.
λ: Ratio of average to maximum crack spacing/width.</td></tr>
<tr><td>BS EN 1992-1-1 (2023)
$s_{x,y\ avg} = 1.5\ c + \frac{k_{fl} \cdot \mathrm{k_b}}{7.2} \frac{d_b}{\rho_{s,\text{eff}}}$</td></tr>
<tr><td>Kaufmann & Marti (1998) / CMM
$s_{x,y\ ,max} = \frac{1}{4} \frac{d_b\left(1 - \rho_{s,\text{eff}}\right)}{\rho_{s,\text{eff}}}$</td><td rowspan="2">$s_{\theta,max} = \frac{\lambda}{\left(\frac{sin\ \theta_{cr}}{s_{x,max}} + \frac{cos\ \theta_{cr}}{s_{y,max}}\right)}$</td><td rowspan="2">$w_{avg} = \lambda\ s_{\theta,max}\ \varepsilon_1$</td></tr>
<tr><td>Adapted AS 3600 model
$s_{x,y\ ,max} = 3.4\ c + 0.3\ k_1 k_2 \frac{d_b}{\rho_{s,\text{eff}}}$</td></tr>
</table>

Most of the reviewed shear panel experiments suffice to report only the average crack widths, which limits the scope of this study to evaluating average cracking behaviour. Consequently, only crack width models that predict average values are directly applicable without modification. Among the considered models, the MCFT and Eurocode provide average crack width models that can be used as is. In contrast, the CMM and the AS3600 are characteristic models and, thus, require further adjustments to align with experimental data. The CMM, for example, estimates the maximum crack spacing, which is often converted to the average value using a modification factor (26). In this study, a factor of $\lambda = 0.69$ is adopted following a statistical analogy of crack spacing distribution to "Rényi's Parking Problem" (27), consistent with recent developments in the CMM framework (28).

Further, the provisions in AS3600 are specifically applicable to flexural and tensile cracking. To extend these provisions to diagonal shear cracks, a pure tensile strain profile is assumed. This assumption enables the calculation of directional crack spacing parameters (longitudinal and transverse), which are then combined trigonometrically, similar to the MCFT, to determine the characteristic spacing of diagonal cracks. The original CEB-FIP formulations, which underpin the Australian code, have historically used a factor of 1.7 to convert average crack spacing to characteristic cracking behaviour (29). Accordingly, this study applies a conversion factor of $\lambda = 1/1.7 \approx 0.59$ to the characteristic AS3600 model. This ratio is deemed appropriate due to the uniform strain distribution observed in panel elements that form comparable distributions for crack widths and spacings.

3. RESULTS AND DISCUSSION

With the modifications presented above, the selected prediction models are evaluated against load stages representative of the serviceability limit state in HSS-reinforced elements. While the selection of these load stages involves an iterative analysis based on a semi-analytical shear framework, the final data used for both estimating and comparing crack widths are entirely empirical in nature. This provides a basis for the experimental validation of existing shear crack width models in the context of transverse high-strength steel (HSS) reinforcement. Figure 1 summarises the performance of selected models by comparing experimentally observed average crack widths with predicted values.

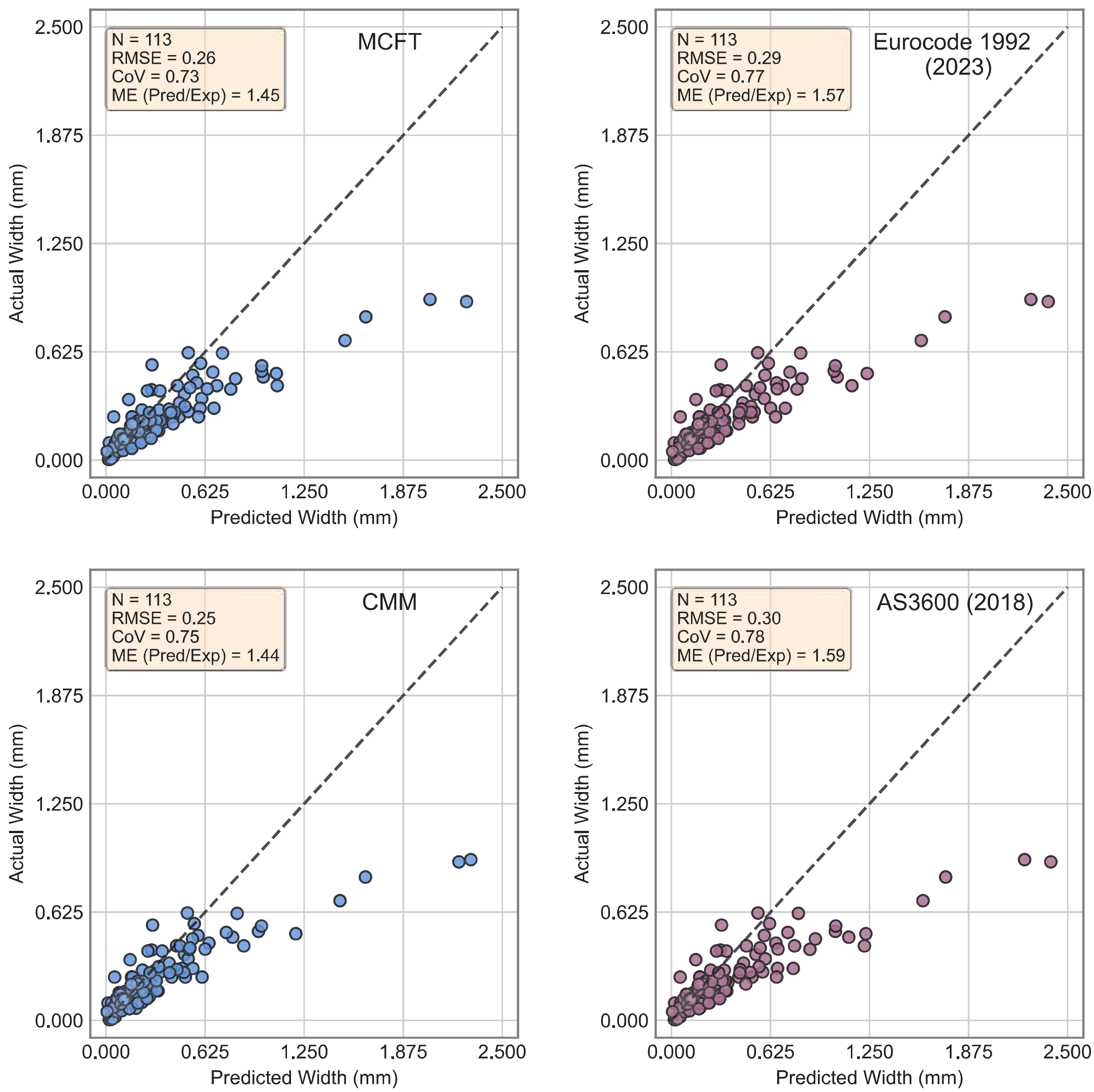

Figure 1. Performance of existing models in predicting SLS diagonal crack widths of RC panels with high-strength transverse reinforcement.

Across all models, crack widths are consistently overestimated for HSS-equivalent panel elements. The mean model error (ME) – defined as the ratio of predicted to experimental values – indicates an average overestimation of roughly 44% in the MCFT and CMM, and up to 57% in design code models. The magnitude of this error, as indicated by the root-mean-squared-error (RMSE), is observed to be at least 0.25 mm, which is roughly the average width observed in an element whose characteristic crack width has reached the limiting threshold (0.4 mm) commonly used in design standards (6,8). With a mean error as large as the serviceability limit, the models further exhibit relatively dispersed predictions as reflected by the coefficient of variation (CoV), underscoring inconsistency in model performance.

Overall, the results suggest that existing models are insufficient in capturing the variation in experimental shear crack widths adequately. These findings for panels are consistent with the similar study involving beam elements with HSS stirrups (9), which confirms that existing models are systematically over-conservative for service shear design of members with HSS transverse steel. Consequently, this could hinder the practical use of high-strength steel as stirrups, since the overestimated crack widths would suggest a serviceability disadvantage compared to mild steel.

The consistent overestimation, as evident in roughly similar mean model errors (MEs), may be partly attributed to the original calibration of these formulations. Although the evaluated semi-analytical models have been extended to diagonal cracking, they were primarily developed and validated using flexural and tensile crack data. To improve their applicability, a similar calibration may be performed using experimental data on diagonal crack widths. However, any scalar adjustment imposed on average width models must account for the distribution of crack widths within an element to be compatible with characteristic width formulations relevant to the design. In the absence of distributed cracking data in the reviewed studies, alternative methods, such as those outlined in reference (30), are recommended to capture a comprehensive distribution of diagonal shear cracking for calibration and modelling purposes.

4. CONCLUSIONS

Concrete structures reinforced with high-strength steel (HSS) offer advantages by reducing material costs and environmental impact. However, major design standards such as AS3600 and ACI 318 do not provision the use of HSS as transverse reinforcement, lacking a reliable crack width prediction model for shear-critical elements. Studies on existing models have shown a tendency to overestimate shear crack widths in beams with HSS stirrups, raising serviceability concerns that limit the practical adoption of HSS in design.

To more accurately evaluate the performance of existing models and investigate potential improvements, this study focuses instead on reinforced concrete panel elements subjected to pure shear loading. These panels eliminate the confounding influence of flexure, offering a more precise assessment of diagonal cracking behaviour. To this end, a dataset comprising over 150 load-crack data points recorded across 47 panel experiments is compiled from the literature. Further, an iterative analysis is employed to identify load stages corresponding to the serviceability limit state of HSS-reinforced elements, thereby avoiding the need for extensive testing. The findings confirm that even under pure shear conditions, existing models overestimate the average diagonal crack widths by at least 44%, indicating a conservative bias. This observed overestimation underscores the need for a refined diagonal crack width model that considers high-strength steel reinforcement.

5. ACKNOWLEDGEMENT

This study is supported through an International PhD Scholarship provided by the University of New South Wales and a research support scholarship by the American Australian Association. This support is acknowledged with thanks.

6. REFERENCES

1. Raoul, J. (2005). *Use and application of high-performance steels for steel structures* (Vol. 8). IABSE.
2. Stroetmann, R. (2011). High strength steel for improvement of sustainability. *Proceedings of the 6th European Conference on Steel and Composite Structures, Proceedings*, *100*, 31.
3. Ng, A., McGregor, G., & Merrick, J. (2023). The curvilinear stress block—A design model to decarbonize reinforced concrete columns using 600 MPa steels. *Australasian Structural Engineering Conference: ASEC 2022*, 27–36. https://doi.org/10.3316/informit.837266895457873

4. Sansom, M., & Lawson, M. (2021). *Life cycle assessment and life cycle costing comparisons of HSS and S355 designs* (D5.1; Stronger Steels in the Built Environment). The Steel Construction Institute.
5. Ban, H., & Shi, G. (2018). A review of research on high-strength steel structures. *Proceedings of the Institution of Civil Engineers-Structures and Buildings*, *171*(8), 625–641.
6. ACI. (2022). *ACI CODE-318-19(22): Building Code Requirements for Structural Concrete and Commentary (Reapproved 2022)*.
7. ACI 439.6R. (2019). *ACI PRC-439.6-19: Guide for the Use of ASTM A1035/A1035M Type CS Grade 100 (690) Steel Bars for Structural Concrete*.
8. AS3600. (2021). *AS 3600:2018 Concrete structures, Amd 2:2021*.
9. Foster, S. J., Parvez, A., Bentz, E., Ng, A., & McGregor, G. (2023). *A Model for the Calculation of Shear Crack Widths for Beams Constructed using High Strength Steel Stirrups*.
10. Xie, L. (2010). *The influence of axial load and prestress on the shear strength of web-shear critical reinforced concrete elements*. University of Toronto.
11. André, H. M. O. (1987). *Toronto/Kajima study on scale effects in reinforced concrete elements*.
12. Beck, A., & Kaufmann, W. (2018). Paradigms of Shear in Structural Concrete—Review and Experimental Verification. In D. A. Hordijk & M. Luković (Eds.), *High Tech Concrete: Where Technology and Engineering Meet* (pp. 684–692). Springer International Publishing. https://doi.org/10.1007/978-3-319-59471-2_81
13. Chintrakarn, R. (2001). *Minimum shear steel and failure modes diagram of reinforced concrete membrane elements* [PhD Thesis]. University of Houston.
14. Pang, X.-B. D., & Hsu, T. T. (1995). Behavior of reinforced concrete membrane elements in shear. *Structural Journal*, *92*(6), 665–679.
15. Proestos, G. T., Bae, G.-M., Cho, J.-Y., Bentz, E. C., & Collins, M. P. (2016). Influence of high-strength bars on shear response of containment walls. *ACI Structural Journal*, *113*(5), 917–928.
16. Susetyo, J., Gauvreau, P., & Vecchio, F. J. (2011). Effectiveness of Steel Fiber as Minimum Shear Reinforcement. *ACI Structural Journal*, *108*(4).
17. Vecchio, F. J., Collins, M. P., & Aspiotis, J. (1994). High-strength concrete elements subjected to shear. *ACI Structural Journal-American Concrete Institute*, *91*(4), 423–433.
18. Vecchio, F. J., & Chan, C. C. L. (1990). Reinforced Concrete Membrane Elements with Perforations. *Journal of Structural Engineering*, *116*(9), 2344–2360. https://doi.org/10.1061/(ASCE)0733-9445(1990)116:9(2344)
19. Vecchio, F. J., & Collins, M. P. (1986). The modified compression-field theory for reinforced concrete elements subjected to shear. *ACI J.*, *83*(2), 219–231.
20. Xie, L., Bentz, E. C., & Collins, M. P. (2011, November 1). *Influence of Axial Stress on Shear Response of Reinforced Concrete Elements. | EBSCOhost*. https://doi.org/10.14359/51683373
21. Meyboom, J., & Marti, P. (2001). *Experimental investigation of shear diaphragms in reinforced concrete slabs* (p. 165 S.). ETH Zurich. http://hdl.handle.net/20.500.11850/145661
22. Khalifa, J. U. (1987). *Limit analysis and design of reinforced concrete shell elements*. University of Toronto.
23. Collins, M. P., & Mitchell, D. (1997). *Prestressed concrete structures*. Response Publications.
24. Kaufmann, W., & Marti, P. (1998). Structural Concrete: Cracked Membrane Model. *Journal of Structural Engineering*, *124*(12), 1467–1475. https://doi.org/10.1061/(ASCE)0733-9445(1998)124:12(1467)
25. BS EN 1992. (2023). *Design of Concrete Structures* (1992-1–1).
26. Kaufmann, W., & Mata-Falcón, J. (2017). Crack widths in structural concrete subjected to in-plane loading. *Proc., Crack Width Calculation Methods for Large Concrete Structures*, 21–25.
27. Murray, A., Gilbert, R. I., & Castel, A. (2018). Spacing of Cracks in Reinforced Concrete Based on a Variable Transfer Length Model. *Journal of Structural Engineering*, *144*(7), 04018090. https://doi.org/10.1061/(ASCE)ST.1943-541X.0002095
28. Gehri, N., Mata-Falcón, J., & Kaufmann, W. (2025). Cracked Membrane Model for Strain-Softening Fiber-Reinforced Concrete. *Journal of Structural Engineering*, *151*(1), 04024190. https://doi.org/10.1061/JSENDH.STENG-13524
29. CEB-FIP. (1978). *CEB-FIP Model Code for Concrete Structures 1978*. T. Telford.
30. Hagh, M., Foster, S., & Vali Pour, H. (2024). A Computer Vision Method to Measure Distribution of Crack Characteristics in Reinforced Concrete Elements. *Proc. of the 15th Fib International PhD Symposium in Civil Engineering*, 349–356.

7. APPENDIX – SLS ITERATIVE ANALYSIS PROCEDURE FOR RC PANELS

Step 1: Calculate the shear stress at SLS: Say, $v_{service} \in [0.4\, V_{nominal}, 0.6\, V_{nominal}]$.

Step 2: Calculate longitudinal strain, $\varepsilon_{x,service}$ that corresponds to SLS with an initial guess of $\varepsilon_{x,nominal}$.

$$s_{xe} = \frac{35\, s_x}{a_g\ + 16} \leq 300 \tag{1}$$

$$\beta = \frac{0.4}{1 + 1500\varepsilon_x} \cdot \frac{1300}{1000 + s_{xe}} \tag{2}$$

$$\theta_v = (29° + 7000\varepsilon_x)\left(0.88 + \frac{s_{xe}}{2500}\right) \leq 75° \tag{3}$$

$$f_{c1} = \frac{\beta\sqrt{f_c'}}{\cot\theta_v} \tag{4}$$

$$\varepsilon_x = \frac{v_{service}\cot\theta_v - f_{c1}}{\rho_x E_s}\text{, assuming } \varepsilon_{sx} \approx \varepsilon_{cx} = \varepsilon_x \tag{5}$$

Step 3: Estimate a value for concrete principal tensile strain, ε_{c1}.

$$\varepsilon_{c1} \approx \varepsilon_x + 5 * 10^{-4} \tag{6}$$

Step 4: Calculate principal tensile stress, f_{c1} and ensure compatibility with MCFT's "crack check".

$$f_{c1} = \begin{cases} \dfrac{0.33\sqrt{f_c'}}{1 + 500\varepsilon_{c1}}, & \varepsilon_{c1} \geq f_{ct}/E_c \\ E_c * \varepsilon_{c1}, & \varepsilon_{c1} < f_{ct}/E_c \end{cases} \tag{7}$$

Step 5: Estimate stress in transverse steel, f_{sz}. An initial guess may be used to start the iteration.

Step 6: Calculate shear contribution of concrete and steel. An initial guess may be used to estimate stress in transverse steel, f_{sz}.

$$v_{steel} = \rho_{sz}\, f_{sz} \cot(\theta_v) \tag{8}$$

$$v_{concrete} = f_{c1} \cot(\theta_v) \tag{9}$$

$$v_{total} = v_{steel} + v_{concrete} \tag{10}$$

Step 7: Calculate principal compressive stress, f_{c2}.

$$f_{c2} = [\tan(\theta_v) + \cot(\theta_v)]\, v_{total} - f_{c1} \tag{11}$$

Step 8: Calculate the crushing strength of concrete considering compression softening effects.

$$f_{c2.max} = \frac{f_c'}{0.8 + 170\, \varepsilon_{c1}} \tag{12}$$

Step 9 [Condition]: Check that the calculated principal compressive stress, f_{c2} is below the crushing limit of concrete $f_{c2.max}$. If $f_{c2} \leq f_{c2.max}$, continue to step 10. If $f_{c2} > f_{c2.max}$, the concrete fails with the assumed ε_{c1}; go to step 3 and reduce ε_{c1}.

Step 10: Calculate/update principal and longitudinal strains.

$$\varepsilon_{c2} = 0.002\,(1 - \sqrt{1 - \frac{f_{c2}}{f_{c2.max}}} \tag{13}$$

$$\varepsilon_x = \frac{v_{service}\, cot\theta_v - f_{c1}}{\rho_x E_s} \tag{14}$$

$$\varepsilon_{c1} = \varepsilon_x(1 + \cot^2(\theta_v)) + \varepsilon_{c2}\, \cot^2(\theta_v) \tag{15}$$

Step 11 [Condition]: Check if principal tensile strains calculated in steps 10 and 3 equal to a certain tolerance. If $\varepsilon_{c1\,(10)} = \varepsilon_{c1\,(3)}$, continue to Step 12. If $\varepsilon_{c1\,(10)} \neq \varepsilon_{c1\,(3)}$, let $\varepsilon_{c1} = \varepsilon_{c1\,(10)}$ and repeat Steps 4 to 11. Iterate until the calculated strains are within a selected tolerance.

Step 12: Calculate transverse steel strain and stress.

$$\varepsilon_z = \frac{\varepsilon_{c_1} - \varepsilon_{c2}\; tan^2(\theta_v)}{1 + tan^2(\theta_v)} \tag{16}$$

$$f_{sz} = E_s\, \varepsilon_z \leq f_{szy} \tag{17}$$

Step 13 [Condition]: Check if transverse steel stresses calculated in steps 12 and 5 are equal to a certain tolerance. If $f_{sz\,(12)} = f_{sz\,(5)}$, continue to Step 14. If $f_{sz\,(12)} \neq f_{sz\,(5)}$, let $f_{sz} = f_{sz\,(12)}$ and repeat Steps 5 to 12. Iterate until the calculated steel stresses are within a selected tolerance.

Step 14 [Condition]: Check equilibrium and whether the desired external load is resisted. If $v_{service\,(1)} = v_{total\,(6)}$, continue to Step 14. If $v_{service\,(1)} \neq v_{total\,(6)}$, repeat Steps 6 to 14 with a new estimate for θ_v. Iterate until the calculated shear stresses are within a selected tolerance.